NOVEL GEOMAGNETIC FIELD MORPHOLOGICAL CRITERIA AND BOUNDS

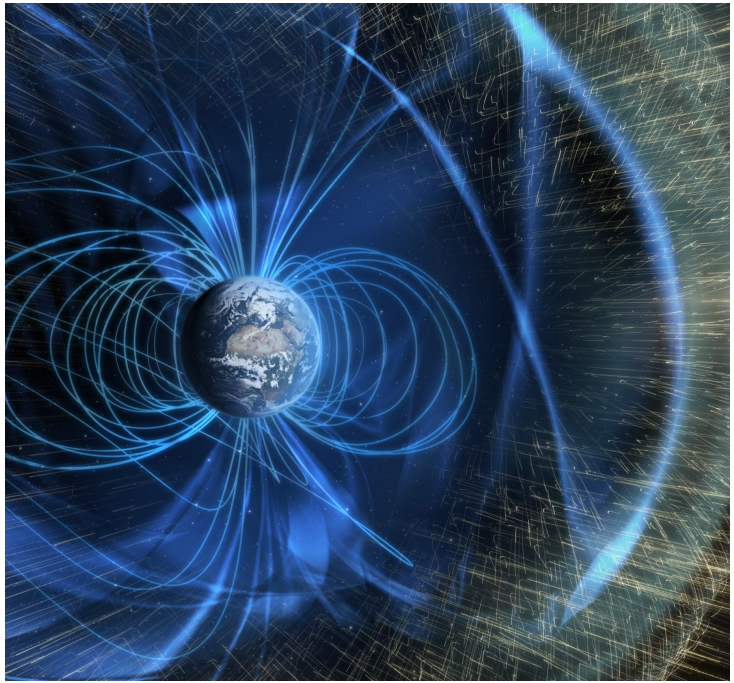

Presented by
Dr. Filipe **TERRA-NOVA** (ANR-POSDOC)
in
ANR DYRE-COMB meeting III, Strasbourg 2025

Terra-Nova, F., Wardinski, I., Panovska, S., Korte, M., Novel geomagnetic field morphological criteria and bounds. JGR: Solid Earth, (in Review).

USP Nantes Université LPG cnes Ecole et Observatoire des Sciences de la Terre anr GFZ Helmholtz-Zentrum Potsdam

CONTEXT

Geomagnetic field models

Limited by data availability and theory adequacy

Numerical dynamo simulations

Wrong input! However, some right output!

Geomagnetic field models

Limited by data availability and theory adequacy

Numerical dynamo simulations

Wrong input! However, some right output!

How to measure the Earth-likeness of a numerical dynamo simulations?

Kinematic	The transport of field by the flow
Dynamical	Force balance inside the outer core
Morphological	The spatial semblance

How to measure the Earth-likeness of a numerical dynamo simulations?

Kinematic	The transport of field by the flow
Dynamical	Force balance inside the outer core
Morphological	The spatial semblance

CLASSICAL CRITERIA

Classical criteria of geomagnetic field morphology

Axial dipolarity
(Glatzmaier et al., 1999)

Equatorial symmetry
(Coe and Glatzmaier, 2006)

Zonality
(Christensen et al., 2010)

Flux concentration
(Christensen et al., 2010)

Four criteria **to evaluate** the **Earth likeness** of numerical dynamo simulations
(Christensen et al. 2010)

Classical criteria of geomagnetic field morphology

Axial dipolarity at the CMB
(Glatzmaier et al., 1999)

$$\mathrm{AD/NAD} = \frac{(g_1^0)^2}{(g_1^1)^2 + (h_1^1)^2 + \sum_{\ell=2}^{\ell_{max}} \left(\left(\frac{a}{c}\right)^{2\ell-2} \left(\frac{\ell+1}{2}\right) \sum_{m=0}^{\ell} (g_\ell^m)^2 + (h_\ell^m)^2 \right)}$$

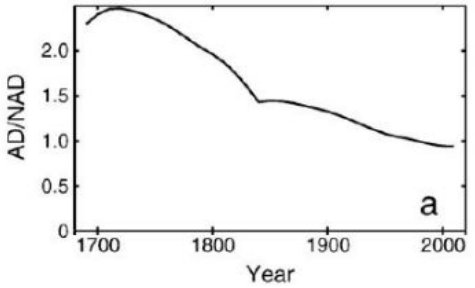

Christensen et al. (2010)

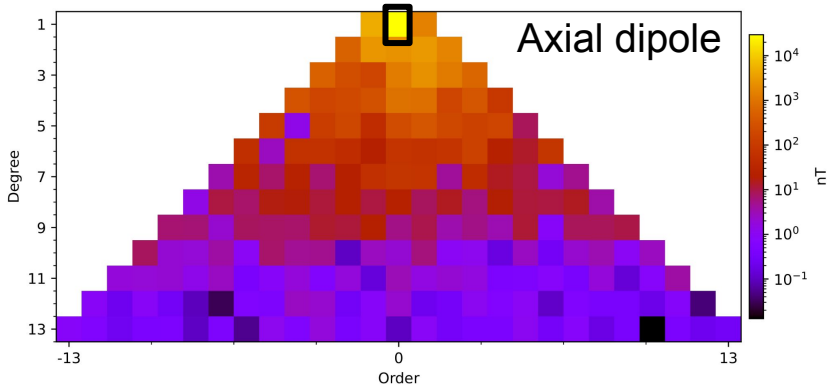

Present-day power spectrum (Finlay et al., 2020)

- **Present-day** field **dipole dominated**
- The **lowest** values of **AD/NAD** (< 10-2) are found in periods of **transitional field** (reversals, excursion)

Classical criteria of geomagnetic field morphology

Equatorial symmetry at the CMB
(Coe and Glatzmaier, 2006)

$$O/E = \frac{\sum_{\ell=2}^{\ell_{max}} \left((\ell+1) \left(\frac{a}{c}\right)^{2\ell+4} \sum_{m=0}^{\ell} \left((g_\ell^m)^2 + (h_\ell^m)^2 \right) \right) \text{ if } \ell + \text{m odd}}{\sum_{\ell=2}^{\ell_{max}} \left((\ell+1) \left(\frac{a}{c}\right)^{2\ell+4} \sum_{m=0}^{\ell} \left((g_\ell^m)^2 + (h_\ell^m)^2 \right) \right) \text{ if } \ell + \text{m even}}$$

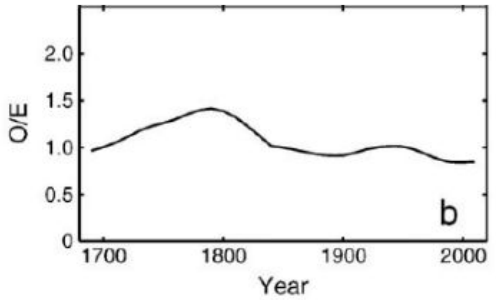

Christensen et al. (2010)

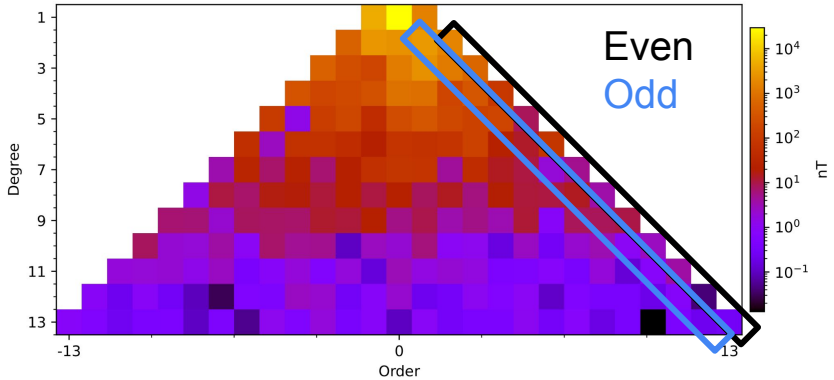

Present-day power spectrum (Finlay et al., 2020)

- For an average of 10000 random equipartitioned magnetic field with ℓmax = 5, 8 and 13, O/E is 0.806, 0.818 and 0.841
- **Larger values than equipartitioned ➪ Equatorial Anti-symmetry**

Classical criteria of geomagnetic field morphology

Zonality at the CMB
(Christensen et al., 2010)

$$Z/NZ = \frac{\sum_{\ell=2}^{\ell_{max}} \left((\ell+1) \left(\frac{a}{c}\right)^{2\ell+4} \left((g_\ell^0)^2 + (h_\ell^0)^2 \right) \right)}{\sum_{\ell=2}^{\ell_{max}} \left((\ell+1) \left(\frac{a}{c}\right)^{2\ell+4} \sum_{m=1}^{\ell} \left((g_\ell^m)^2 + (h_\ell^m)^2 \right) \right)}$$

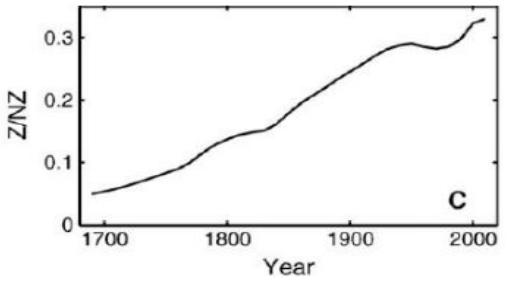

Christensen et al. (2010)

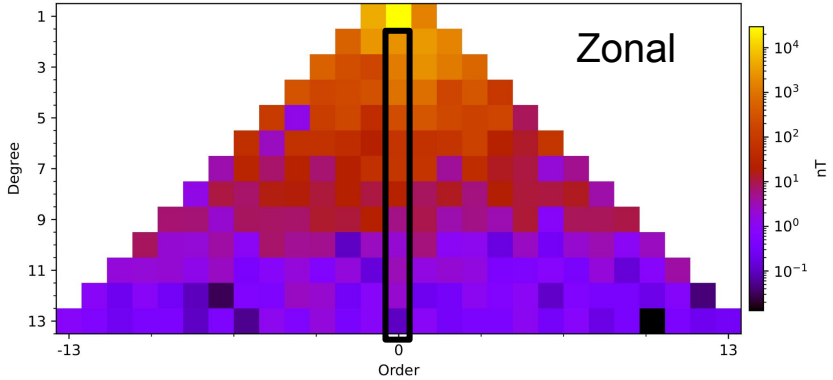

Present-day power spectrum (Finlay et al., 2020)

- For a mean of 10000 random equipartitioned magnetic fields with ℓ_{max} = 5, 8 and 13, Z/NZ is 0.183, 0.145 and 0.112
- **Larger values than equipartitioned ⇨ Field organized in W-E belts**

Classical criteria of geomagnetic field morphology

Flux concentration of the radial field at CMB
(Christensen et al., 2010)

$$\mathrm{FCF} = \frac{\langle B_r^4 \rangle - \langle B_r^2 \rangle^2}{\langle B_r^2 \rangle^2}$$

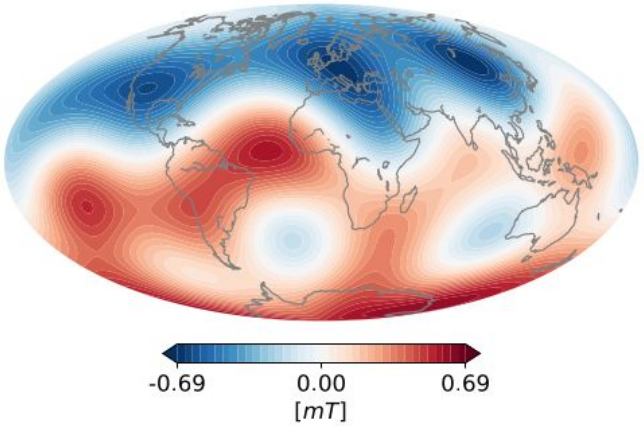

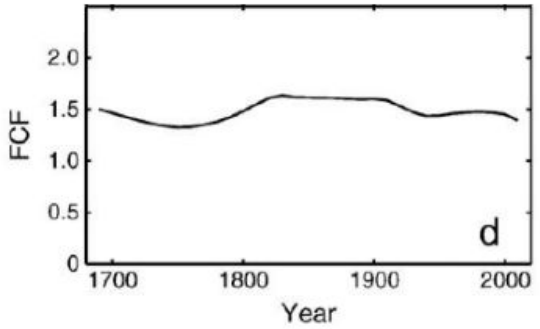

Christensen et al. (2010)

- Pure dipole field: FCF = 0.8 (Christensen et al., 2010)
- With AD/NAD=1.4 and equipartitioned non-dipole field with ℓ_{max} = 8, FCF=1.49 (Christensen et al., 2010)
- The **variance of the Br squared** evaluates the **prominence of flux patches** in the CMB.

Classical bounds for Earth-likeness

Christensen et al. (2010) choice of values based on a **historical field model** (Jackson et al., 2000) truncated at ℓ_{max}**=13**, **archeomagnetic field model** CALS7k.2 ℓ_{max}**=5** (Korte and Constable, 2005) and **paleomagnetic data set** (Tauxe et al., 2007)

However in a non-precise way, e.g.:

Modern field AD/NAD = 1.29
Archeological AD/NAD = 4.00
Paleomagnetic AD/NAD = 2.50

Then AD/NAD bound is 1.40 for Earth-likeness

Christensen et al. (2010) choice of values standard deviation based on **"experience"** ?

$$\sigma_{AD/NAD} = \sigma_{O/E} = 2 \; ; \; \sigma_{Z/NZ} = 2.5; \; \sigma_{FCF} = 1.75$$

Only FCF has a physical meaning

Rating of compliance

Individual score for each criteria by

$$\chi_i^2 = \left(\frac{\ln \Pi_i - \ln \Pi_i^E}{\ln \sigma_i^E} \right)^2$$

Interval for good score ($\chi_i^2 = 1.0$)

$$[\Pi_i^E / \sigma_i^E ; \Pi_i^E \sigma_i^E]$$

Scoring assignment

$$\chi^2 = \sum_i \chi_i^2$$

Quantifying Earth likeness

Level of compliance:

- ➔ $\chi^2 < 2$ *excellent*
- ➔ $2 < \chi^2 < 4$ *good*
- ➔ $4 < \chi^2 < 8$ *marginal*
- ➔ $8 < \chi^2$ *no complicance*

A path towards Earth-Likeness

- **Darker symbols more compliant the numerical dynamos simulations**
- **Earth-likess in the Rm − Eη parameter space is bounded approximately by the broken lines**

(Christensen et al., 2010)

Fixed temperature

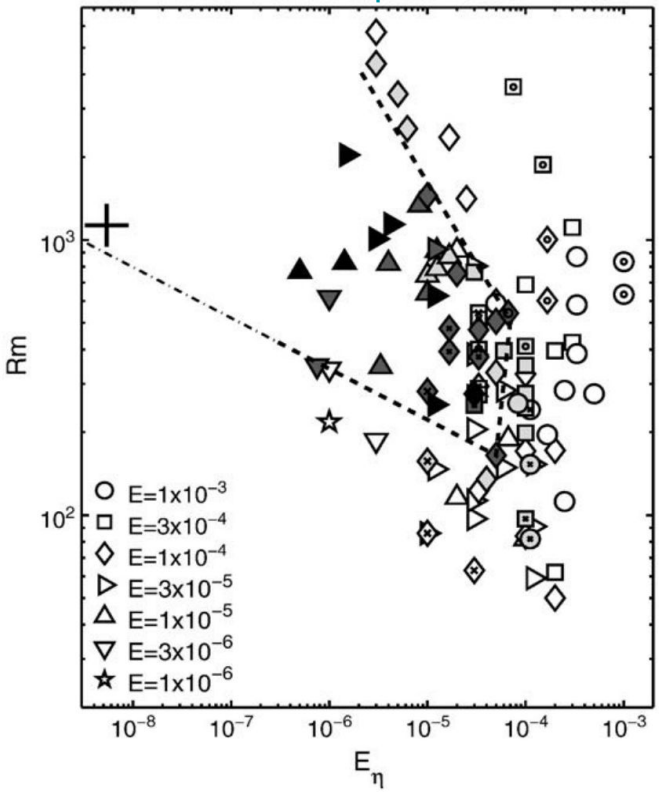

Fixed Flux

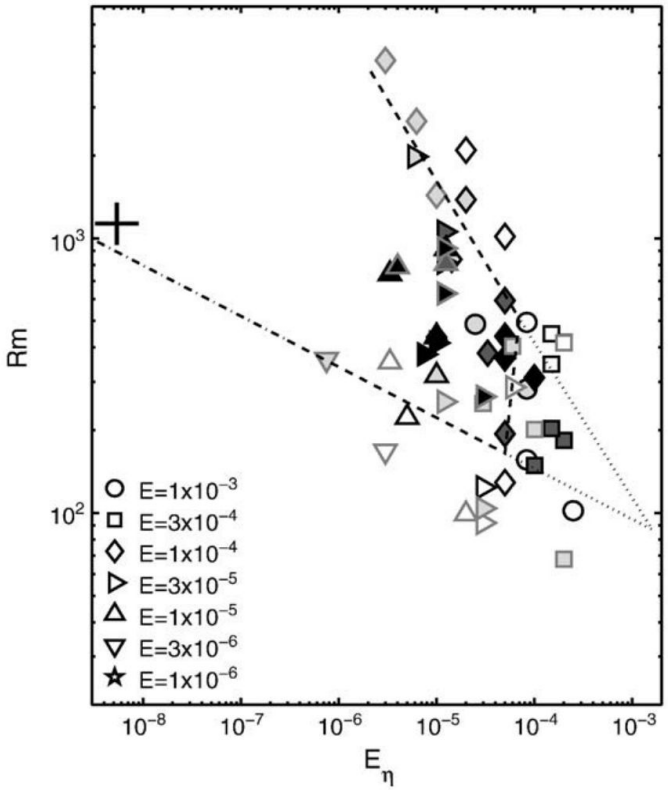

NOVEL CRITERIA

Terra-Nova, F., Wardinski, I., Panovska, S., Korte, M., Novel geomagnetic field morphological criteria and bounds. JGR: Solid Earth, (in Review).

Novel criteria of geomagnetic field morphology

Regions of weak field

Surface intensity field minimum anomaly (F^*_{min})

Mantle control

Flux patch duet (FPD)

Two **auxiliary** criteria to evaluate the Earth likeness of numerical dynamo simulations

Surface intensity field minimum anomaly

Surface intensity field minimum anomaly

How **deep** is the surface **field minimum** in respect to the field everywhere else.

$$F^*_{min} = \frac{F_{min}}{\langle F \rangle}$$

- Pure axial dipole field $F^*_{min} \approx 0.725$
- Constant F, $F^*_{min} = 1.0$ (maximum value)

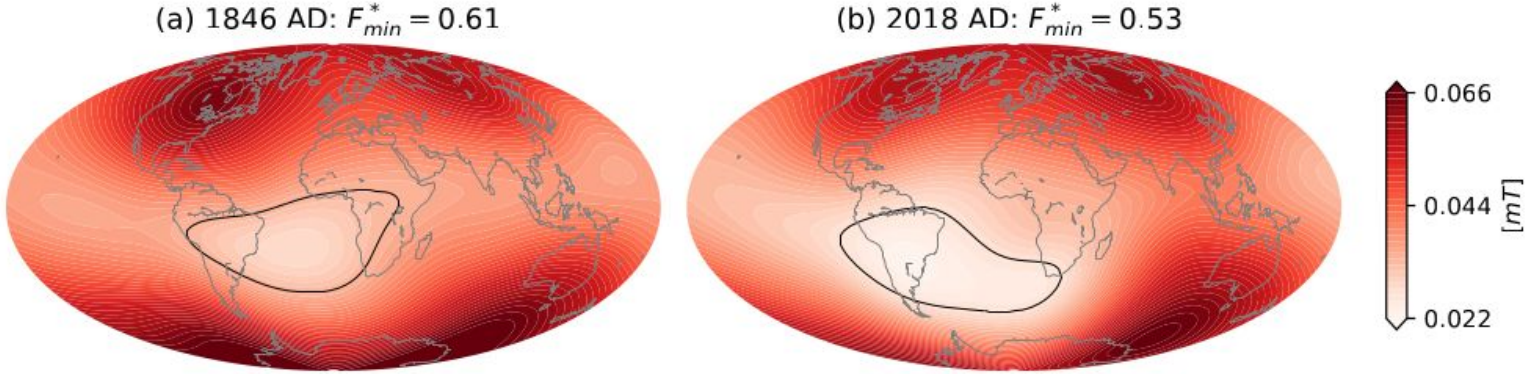

Larger/smaller F^*_{min} implies **smaller/larger** area of $1.2F^*_{min}$ hence **less/more** pronounced surface intensity minimum

Surface intensity field minimum anomaly

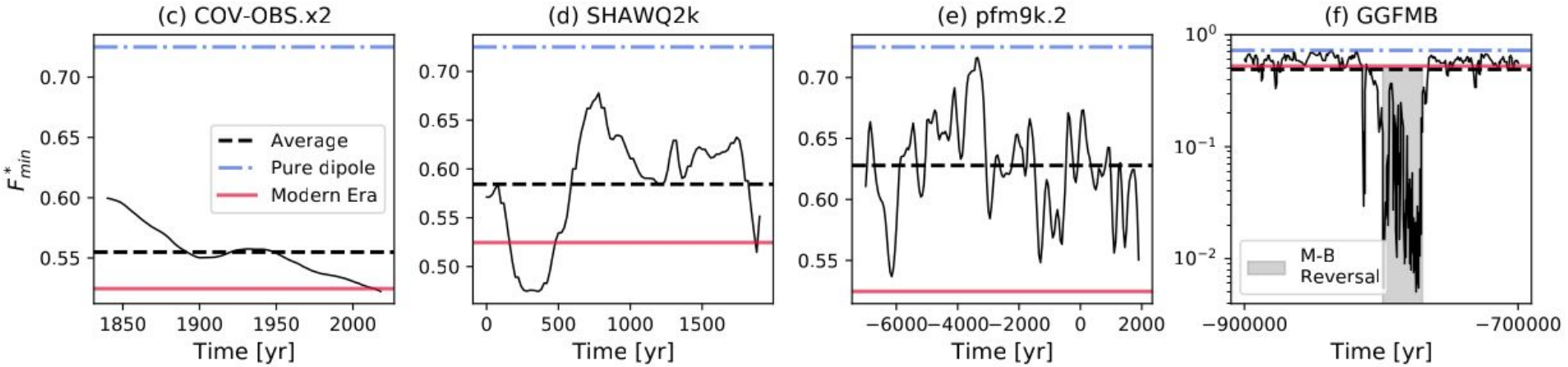

- Minimum getting **more prominent throughout** the **historical** period.
- An episode of a **significant minimum** in the **archaeomagnetism** era model.
- In the **Holocene** model, F^*_{min} is usually **much larger than the modern value**.
- **Extremely low values** of F^*_{min}, O(−2), **during excursions or reversals**.

Flux patch duet

CMB

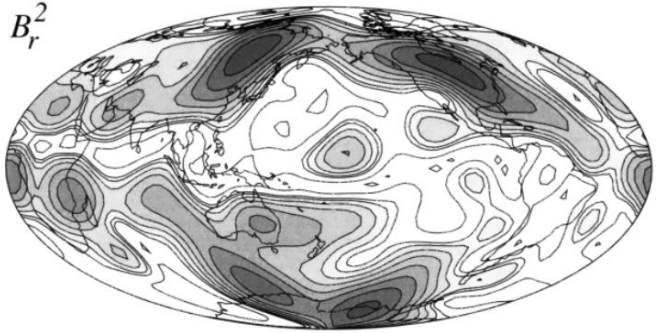

Lowermost mantle

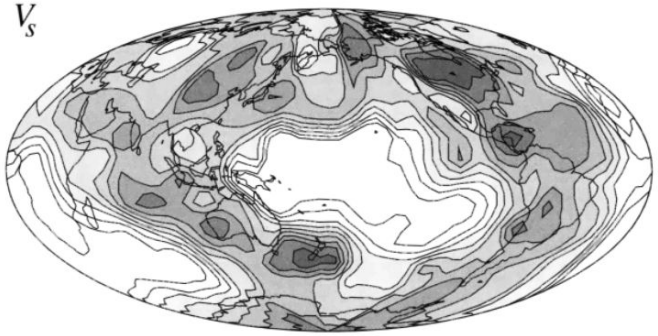

- **Order 2** longitudinal organization of the **radial field structures at the CMB (e.g IGRF-14).**
- **Order 2** dominance in **lowermost mantle tomography models (e.g. Masters et al., 2000).**
- **Phase agreement** (Gubbins, 2003)**.**

Flux patch duet

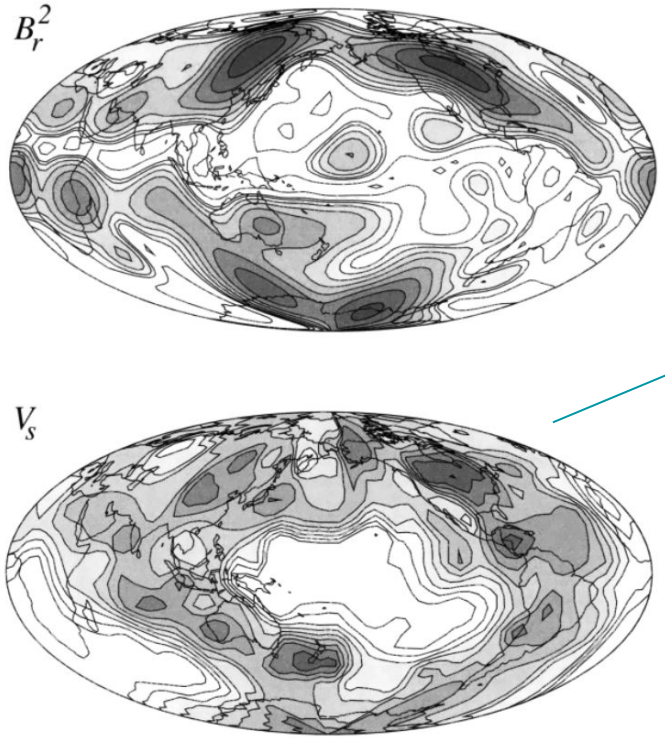

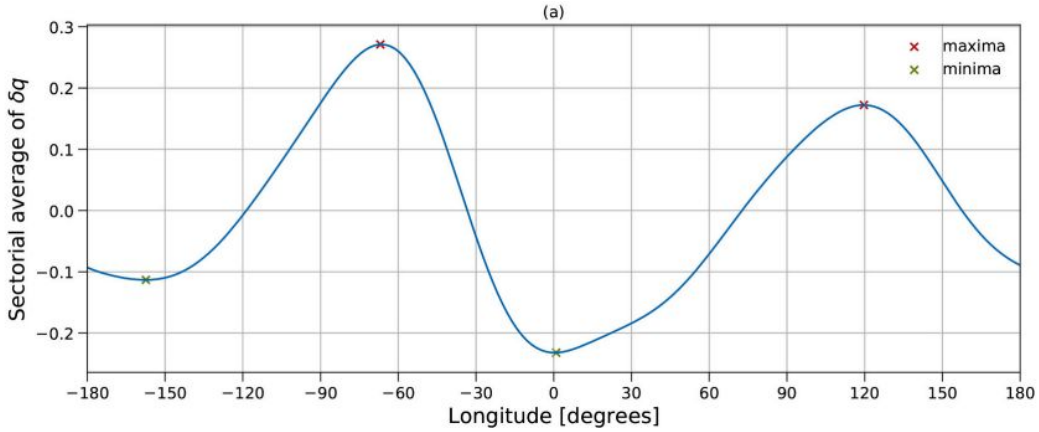

- **Order 2** longitudinal organization of the **radial field structures at the CMB (e.g IGRF-14).**
- **Order 2** dominance in **lowermost mantle tomography models (e.g. Masters et al., 2000).**
- **Phase agreement** (Gubbins, 2003)**.**

Flux patch duet

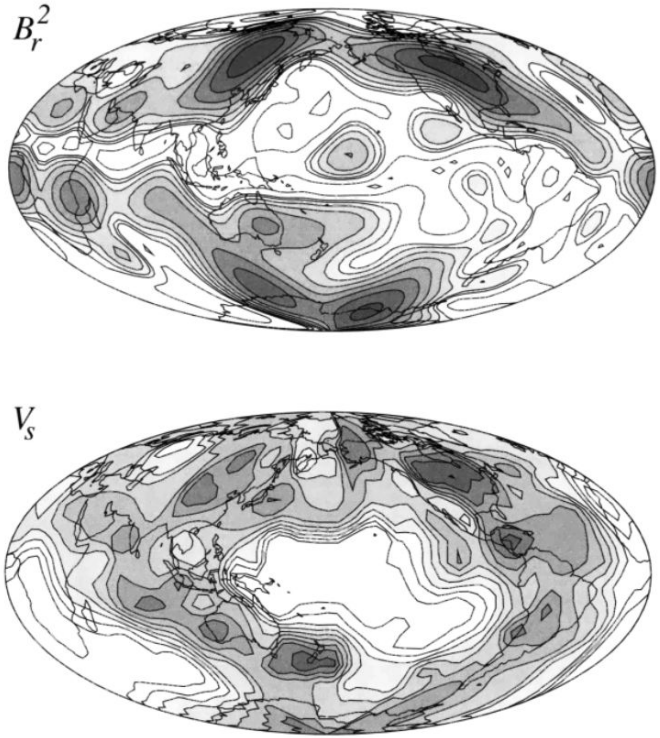

Flux patch duet

1. The latitudinal average of Br squared at the CMB
2. Apply FFT: $$X_j = \sum_{\kappa=0}^{N-1} A_\kappa W^{j\kappa}, j = 0, 1, ..., N-1$$
3. Infer FPD from the FFT amplitude coefficients:

$$\text{FPD} = \frac{A_2}{(A_1 + A_3 + ... + A_{\ell_{max}})/(N-1)}$$

- **Order 2** longitudinal organization of the **radial field structures at the CMB** (e.g IGRF-14)
- **Order 2** dominance in **lowermost mantle tomography models** (e.g. Masters et al., 2000)
- **Phase agreement** (Gubbins, 2003)

Flux patch duet

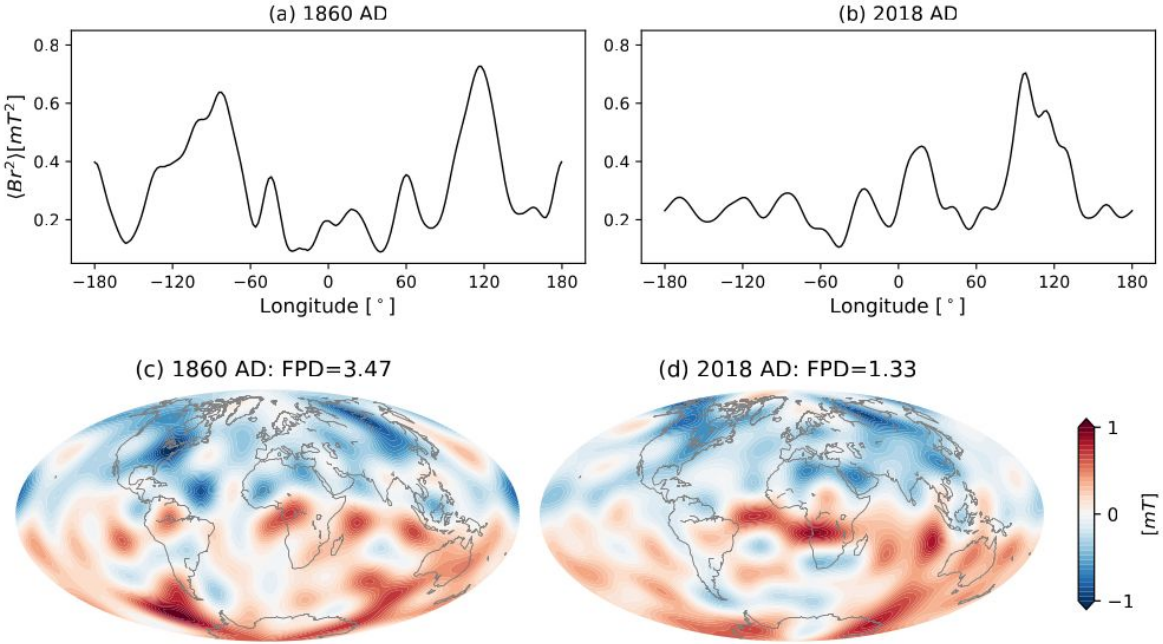

- **Two** antipodal peaks to **one** peak **from 1860 to 2018 AD** where the peak at ≈ 90° W vanished

- FPD time dependence reflects differences in **morphology** in the **Southern hemisphere**

Flux patch duet

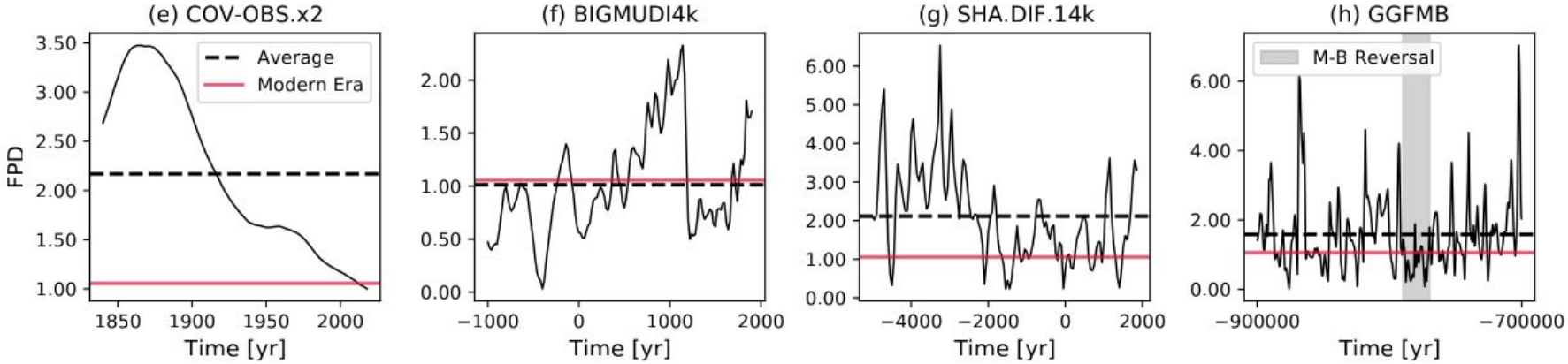

- **FPD** ratio has **continuously decreased** from 1860 AD **until present**
- **Ancient** models have **intermittent large/small FPD**
- **Holocene** has **long episodes of high FPD** value between ≈ 6000 BC and 2200 BC
- The FPD in the **Pleistocene** reaches values **larger than 6.00**

Suite of geomagnetic field models

NOVEL CRITERIA

Model name	Reference	ℓ_{max}	Data type	Modeling	Period	Time interval	Δt
CHAOS7.13	Finlay et al. (2020)	14	St & O	SI	Modern	1997 AD - 2022 AD	1
KALMAG	Baerenzung et al. (2022)	14	St & O & H	BI	Historical	1900 AD - 2016 AD	8
GUFM1	Jackson et al. (2000)	14	O & H	SI	Historical	1840 AD - 1990 AD	2.5
COV-OBS.x2	Huder et al. (2020)	14	St & O & H	BI	Historical	1840 AD - 2018 AD	2
BIGMUDIh.1	Arneitz et al. (2021)	14	O & H & A & L	BI	Historical	1380 AD - 1920 AD	3.5
HistKalmag	Schanner et al. (2023)	14	O & H & A & L	BI	Historical	1000 AD - 1940 AD	10
SHAWQ2k	Campuzano et al. (2019)	10	A & L	SI	Archeological	0000 AD - 1900 AD	20
ARCH3k	Korte et al. (2009)	14	A & L	SI	Archeological	1000 BC - 1900 AD	5
A_FM-M	Licht et al. (2013)	5	A & L	SI	Archeological	1000 BC - 1900 AD	40
ASD_FM-M	Licht et al. (2013)	5	A & L & S	SI	Archeological	1000 BC - 1900 AD	40
ASDI_FM-M	Licht et al. (2013)	5	A & L & S	SI	Archeological	1000 BC - 1900 AD	40
COV-ARCH	Hellio and Gillet (2018)	10	A & L	BI	Archeological	1000 BC - 1900 AD	100
COV-LAKE	Hellio and Gillet (2018)	10	A & L & S	BI	Archeological	1000 BC - 1900 AD	100
BIGMUDI4k	Arneitz et al. (2019)	8	H & A & L	BI	Archeological	1000 BC - 1900 AD	20
SHA.DIF.14k	Pavón-Carrasco et al. (2014)	10	A & L	BI	Holocene	5000 BC - 1850 AD	50
ArchKalmag14k	Schanner et al. (2022)	14	A & L	BI	Holocene	6000 BC - 1900 AD	50
pfm9k.2	Nilsson et al. (2022)	8	A & L & S	BI	Holocene	7000 BC - 1900 AD	10
HFM.OL1.A1	Constable et al. (2016)	10	A & L & S	SI	Holocene	8000 BC - 1900 AD	10
CALS10K.2	Constable et al. (2016)	10	A & L & S	SI	Holocene	8000 BC - 1900 AD	10
LSMOD.2	Korte et al. (2019)	10	A & L & S	SI	Pleistocene	48k BC - 28k BC	50
GGFSS70	Panovska et al. (2021)	6	S	SI	Pleistocene	70k BC - 14k BC	100
GGF100k	Panovska et al. (2018)	10	A & L & S	SI	Pleistocene	100k BC - 1650 BC	200
GGFMB	Mahgoub et al. (2023)	6	S	SI	Pleistocene	900K BC - 700k BC	200

23 geomagnetic field models grouped by ‘epochs’:
1 Modern, **5** historical, **8** Archeological, **5** Holocene and **4** Pleistocene

Time averaged results geomagnetic field models

NOVEL CRITERIA

Model	AD/NAD	O/E	Z/NZ	FCF	F^*_{min}	FPD
Modern						
CHAOS7	1.30(0.01)	0.88(0.01)	0.35(0.00)	1.03(0.02)	0.52(0.00)	1.06(0.06)
Historical era						
KALMAG	1.55(0.24)	0.87(0.02)	0.34(0.01)	1.12(0.06)	0.54(0.01)	1.59(0.42)
GUFM1	1.74(0.25)	0.88(0.07)	0.30(0.05)	1.17(0.06)	0.56(0.02)	2.29(0.79)
COV-OBS.x2	1.69(0.27)	0.89(0.06)	0.31(0.06)	1.17(0.07)	0.55(0.02)	2.17(0.84)
BIGMUDIH.1	2.48(0.44)	0.64(0.13)	0.33(0.13)	1.29(0.15)	0.58(0.03)	0.82(0.50)
HistKalmag	1.95(0.48)	1.09(0.40)	0.21(0.11)	1.21(0.24)	0.58(0.04)	1.72(1.11)
Archeological era						
SHAWQ2k	2.39(0.66)	1.07(0.31)	0.19(0.13)	1.24(0.45)	0.58(0.05)	1.64(1.19)
ARCH3k	3.52(0.74)	0.74(0.30)	0.22(0.15)	1.08(0.21)	0.62(0.03)	1.81(1.07)
A_FM	4.36(1.77)	0.66(0.23)	0.22(0.13)	1.13(0.27)	0.63(0.04)	1.96(0.86)
ASD_FM	3.17(1.17)	1.09(0.47)	0.24(0.16)	1.43(0.22)	0.56(0.04)	1.38(0.78)
ASDI_FM	3.85(1.57)	1.01(0.36)	0.21(0.12)	1.39(0.19)	0.59(0.04)	1.53(0.85)
COV-ARCH	1.91(0.55)	0.86(0.39)	0.27(0.14)	1.23(0.25)	0.61(0.04)	1.61(0.67)
COV-LAKE	1.21(0.37)	0.94(0.51)	0.19(0.17)	1.56(0.18)	0.55(0.07)	1.03(0.60)
BIGMUDI4k	2.26(0.79)	0.56(0.18)	0.37(0.18)	1.05(0.25)	0.56(0.06)	1.01(0.49)
Holocene era						
SHADIF14k	3.19(1.20)	1.04(0.46)	0.11(0.08)	1.27(0.32)	0.61(0.04)	2.11(1.19)
ArchKalMag14k	3.52(2.44)	0.96(0.54)	0.20(0.19)	1.38(0.34)	0.58(0.06)	1.86(1.33)
pfm9k.2	4.79(2.59)	0.79(0.46)	0.28(0.21)	1.30(0.38)	0.63(0.04)	2.02(1.18)
HFM.OL1.A1	4.62(1.92)	1.21(0.65)	0.33(0.26)	1.45(0.30)	0.62(0.04)	1.38(0.79)
CALS10K.2	3.94(1.70)	1.15(0.59)	0.23(0.13)	1.52(0.50)	0.63(0.05)	1.52(0.75)
Pleistocene era						
LSMOD.2	1.57(1.20)	0.80(0.52)	0.26(0.23)	1.75(0.44)	0.48(0.16)	1.58(0.75)
GGFSS70k	2.07(2.05)	1.03(0.68)	0.23(0.24)	1.79(0.65)	0.48(0.15)	1.44(0.97)
GGF100k	2.28(1.23)	0.86(0.58)	0.27(0.21)	1.71(0.48)	0.56(0.09)	1.70(1.03)
GGFMB	1.53(1.51)	0.78(0.46)	0.39(0.35)	2.37(1.15)	0.49(0.20)	1.58(1.04)

23 geomagnetic field models grouped by ‘epochs’:
1 Modern, **5** historical, **8** Archeological, **5** Holocene and **4** Pleistocene

Classical bounds for Earth likeness

	AD/NAD	O/E	Z/NZ	FCF	F^*_{min}	FPD
From Christensen et al. (2010)						
Π_i^E	1.40	1.00	0.15	1.50	-	-
σ_i^E	2.00	2.00	2.50	1.75	-	-

- **Should it be one number for each epoch?**
- **Should the classical values be changed as well?**
- **How to infer new values of acceptable departs from the mean? Still logarithmic differences?**

New bounds for Earth likeness

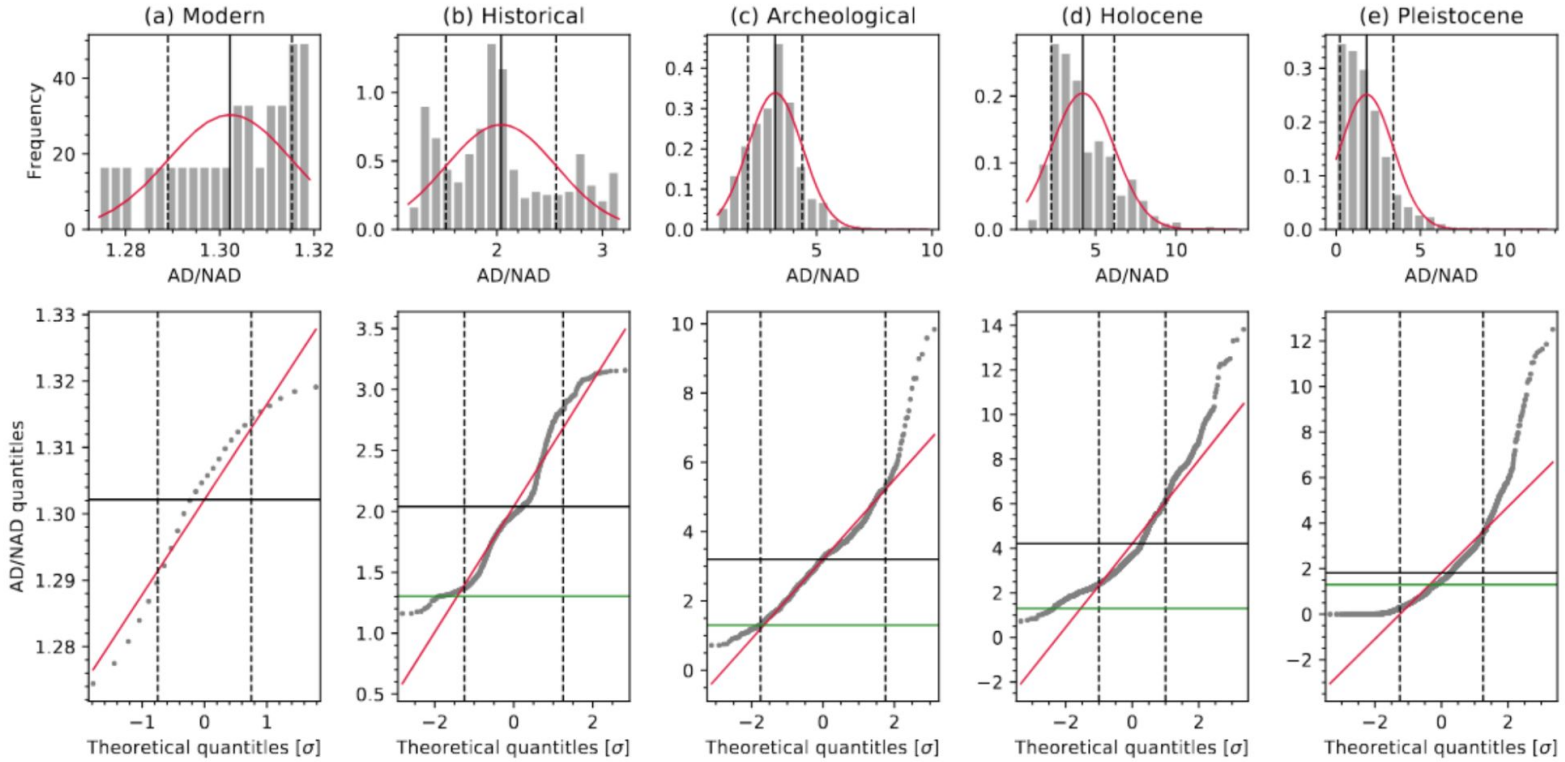

- **How to find the new standard deviation ?**

New bounds and acceptable deviations for Earth-likeness

- **New standard deviations** based on the **statistics** of **all models of a specific era?**

	AD/NAD	O/E	Z/NZ	FCF	F^*_{min}	FPD
From Christensen et al. (2010)						
Π_i^E	1.40	1.00	0.15	1.50	-	-
σ_i^E	2.00	2.00	2.50	1.75	-	-
Modern era truncated at $\ell_{max} = 8$						
Π_i^E	0.94	0.84	0.33	1.39	0.49	1.50
σ_i^E	1.00[a]	1.25	1.00	1.25	1.25	1.25
Modern era truncated at $\ell_{max} = 5$						
Π_i^E	1.30	0.88	0.35	1.03	0.52	1.06
σ_i^E	0.75	0.75	0.75	1.25	1.50	0.75
Historical era						
Π_i^E	2.04	0.84	0.29	1.22	0.57	1.56
σ_i^E	1.25	1.25	2.00	1.75	1.75	1.75
Archeological era						
Π_i^E	3.21	0.79	0.24	1.15	0.60	1.63
σ_i^E	1.75	1.25	1.25	1.25	1.25	1.25
Holocene era						
Π_i^E	4.20	1.13	0.26	1.45	0.62	1.55
σ_i^E	1.00	1.25	1.00	1.50	1.25	1.75
Pleistocene era						
Π_i^E	1.81	0.86	0.29	2.00	0.50	1.58
σ_i^E	1.25	1.25	1.25	1.25	0.75	1.25

[a] from Christensen et al. (2010). Π_i^E is the target value and σ_i^E represents how much the value can depart from its mean to score well

Rating of compliance with present-day field

To quantify the semblance of past fields to the present-day field

- **Weak compliance** of several models of the ancient field built with distinctive periods, data sets and modeling methodologies may suggest a **highly time-dependent geodynamo.**
- **Alternatively**, it may indicate that the models morphological criteria are **limited by their data sets and methodologies.**

Model	$\langle\chi^2\rangle$	$\min(\chi^2)$	τ^2_χ	$\langle\chi'^2\rangle$	$\min(\chi'^2)$	$\tau_{\chi'^2}$
Historical						
KALMAG	0.06	0.00	100/0/0/0	0.54	0.00	100/0/0/0
GUFM1	0.30	0.01	100/0/0/0	1.27	0.07	84/16/0/0
COV-OBS.x2	0.21	0.00	100/0/0/0	0.98	0.00	88/12/0/0
BIGMUDIH.1	1.75	0.29	73/27/0/0	2.83	1.24	81/16/3/0
HistKalmag	1.75	0.12	56/33/6/5	4.29	0.70	45/45/6/3
Archeological						
SHAWQ2k	2.32	0.47	41/32/21/6	7.20	1.24	31/31/27/10
ARCH3k	3.42	0.47	15/49/27/10	6.79	2.15	23/38/23/17
A_FM	4.30	1.25	4/45/38/14	6.71	2.37	8/51/19/22
ASD_FM	3.48	0.26	24/43/28/4	6.70	2.72	16/47/30/7
ASDI_FM	3.99	0.67	18/32/45/5	6.86	4.37	0/61/32/7
COV-ARCH	1.19	0.45	77/17/7/0	4.91	1.28	37/47/17/0
COV-LAKE	3.17	0.65	33/33/33/0	7.55	1.35	17/37/37/10
BIGMUDI4k	1.57	0.43	66/16/18/0	2.76	0.68	72/12/12/5
Holocene						
SHA.DIF.14k	4.80	0.97	12/28/37/23	8.31	1.88	13/36/28/24
ArchKalMag14k	4.23	0.21	18/28/35/20	8.63	0.52	14/27/28/31
pfm9k.2	4.83	0.43	12/22/42/23	8.72	1.86	12/33/29/26
HFM.OL1.A1	5.00	0.42	13/23/49/15	11.19	2.15	1/22/33/43
CALS10K.2	4.28	0.47	15/29/41/15	7.64	1.11	14/40/26/20
Pleistocene						
LSMOD.2	3.96	0.57	15/36/28/21	8.05	1.54	8/42/22/28
GGFSS70	4.90	0.52	14/24/38/24	12.83	0.92	4/20/23/53
GGF100k	3.33	0.32	24/37/33/6	7.43	1.42	15/41/26/18
GGFMB	5.52	0.28	12/24/30/34	11.54	2.03	6/22/25/47

$\langle\chi^2\rangle$ is the time averaged rating of compliance, $\min(\chi^2)$ the minimum χ^2 found for a snapshot and τ^2_χ the percentage (in integer) of snapshots of a model that are excellent/good/marginal/non-compliant with respect to the modern field when considering the classical criteria (Christensen et al., 2010). $'$ indicates that both classical and novel criteria are considered.

Rating of compliance with present-day field

(a) Good old and novel

(b) Good old and bad novel (FPD too small)

(c) Bad old (AD/NAD too large) and good novel

(d) Bad old (Z/NZ too small) and novel (FPD too large)

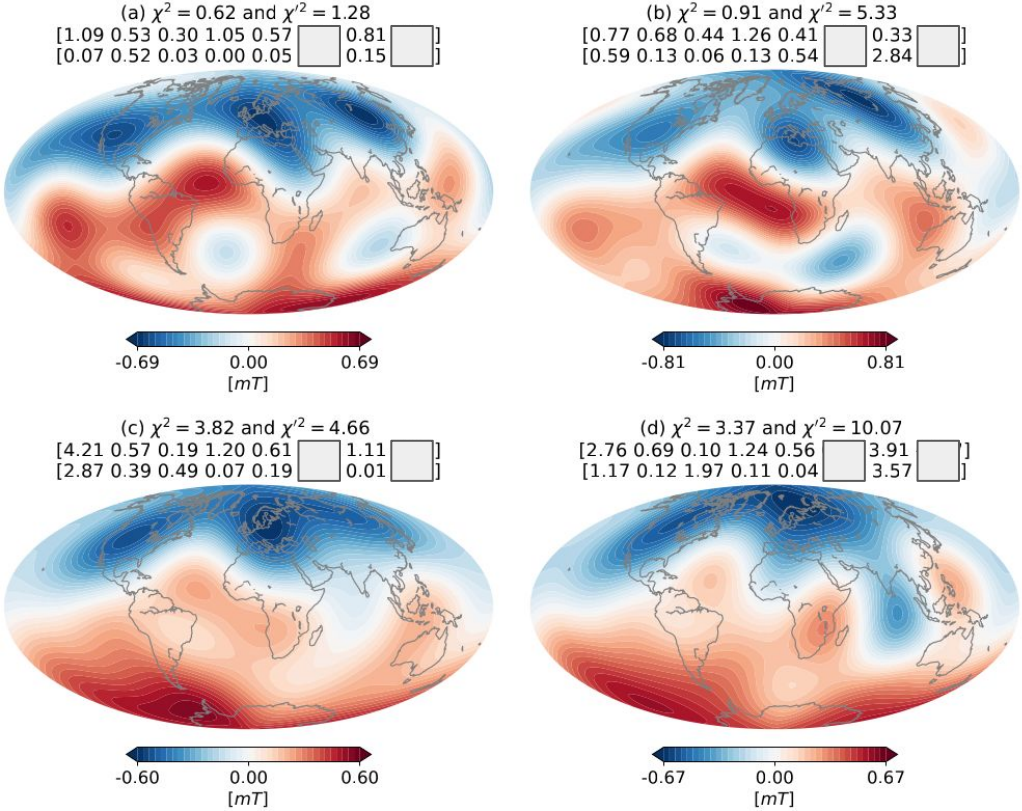

Transitional field

- An excursion if $\theta_{dip} > 45^{\circ}$ (Wicht, 2005)
- Duration of a transitional field is determined by $\max(\theta_{dip}) = 20.43^{\circ}$
- The duration of the Laschamps excursion is ≈ 2400 yr and ≈ 925 yr in LSMOD.2 and GGFSS70, respectively
- $\max(\theta_{dip})=76.30^{\circ}$ in LSMOD.2 and 142.20° in GGFSS70
- The duration of the Matuyama-Brunhes reversal in GGFMB is ≈ 18 kyr

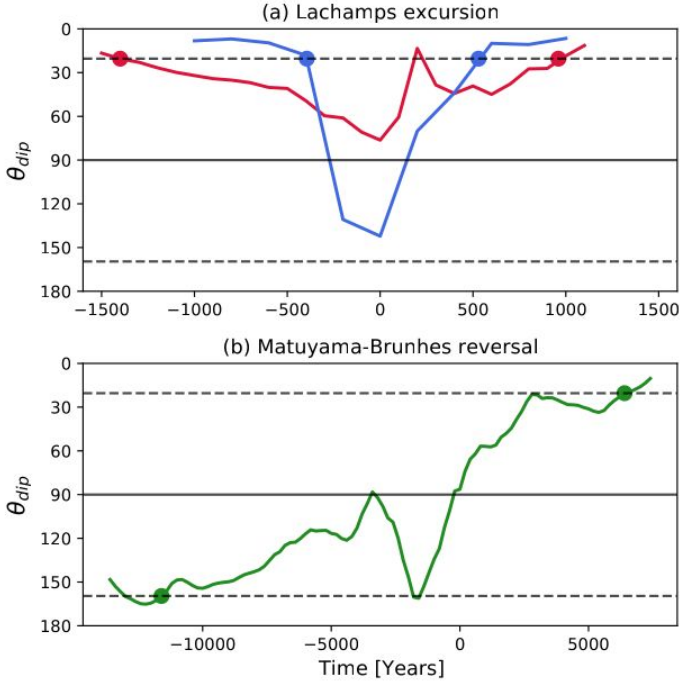

Model	AD/NAD	O/E	Z/NZ	FCF	F^*_{min}	FPD
Laschamps excursion						
LSMOD.2	0.043(0.052)	0.63(0.12)	0.10(0.04)	1.78(0.34)	0.18(0.15)	1.62(0.83)
GGFSS70	0.004(0.004)	0.55(0.09)	0.06(0.04)	3.56(0.81)	0.02(0.02)	1.12(0.19)
Matuyama-Brunhes reversal						
GGFMB	0.028(0.034)	0.73(0.18)	0.20(0.14)	2.14(0.48)	0.06(0.07)	0.73(0.38)

Conclusions

3/6 criteria have significantly larger variations from $\ell_{max} = 5$ (ancient relevant truncation) to $\ell_{max} = 6$ compared to differences between other pairs of successive ℓ_{max} values

Throughout its history the geomagnetic field exhibited intermittent levels of equatorial anti-symmetry and zonality, which may be related to the transient amount of CMB reversed flux

Surface intensity minima can be used as indicators of transitional field

Long-term mantle control on the geodynamo is evident in the recurrent longitudinal pattern of the CMB radial field as well as in the recurrence of stronger northern than southern polar minimum

Conclusions

3/6 criteria have significantly larger variations from $\ell_{max} = 5$ (ancient relevant truncation) to $\ell_{max} = 6$ compared to differences between other pairs of successive ℓ_{max} values

Throughout its history the geomagnetic field exhibited intermittent levels of equatorial anti-symmetry and zonality, which may be related to the transient amount of CMB reversed flux

Surface intensity minima can be used as indicators of transitional field

Long-term mantle control on the geodynamo is evident in the recurrent longitudinal pattern of the CMB radial field as well as in the recurrence of stronger northern than southern polar minimum

Thank you for the attention

Spatial resolution dependence

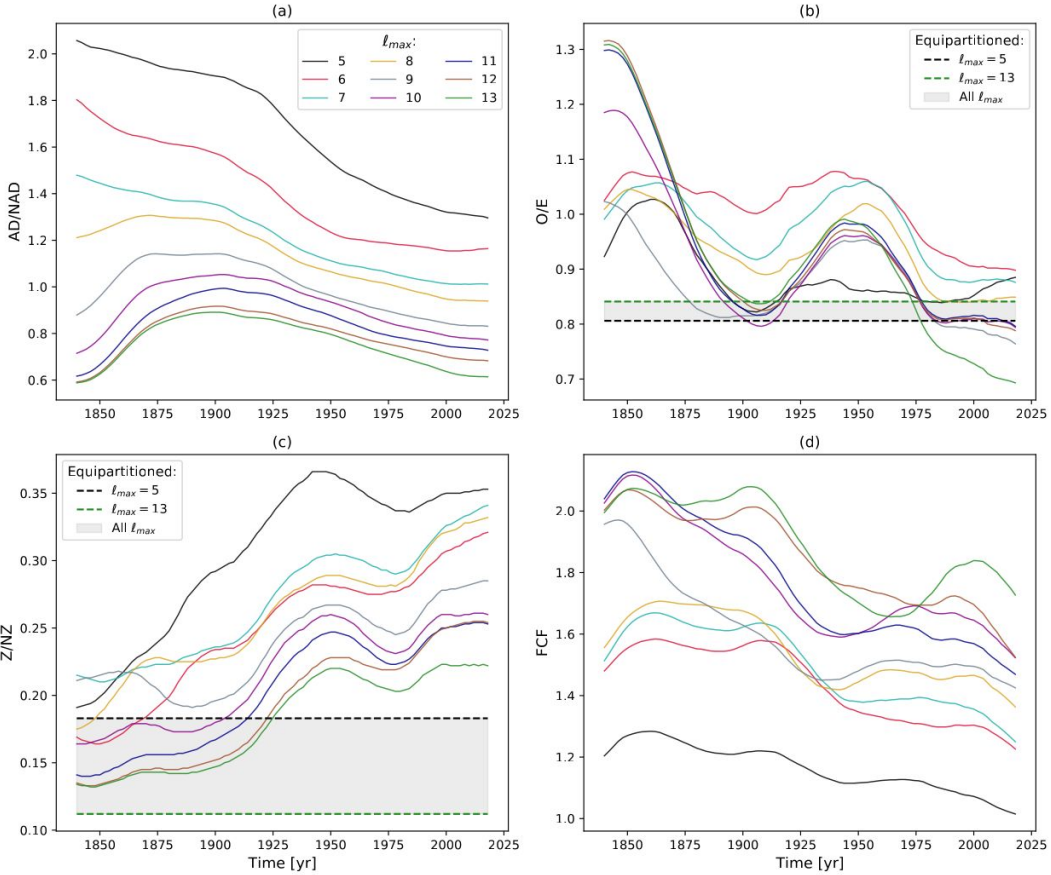

Time-averages:

- AD/NAD value is 0.45 times smaller from ℓmax = 5 to ℓ_{max} = 13
- O/E weakly dependent on ℓ_{max}
- Z/NZ decreases with increasing ℓ_{max}
- FCF increases with increasing ℓ_{max}

Spatial resolution dependence

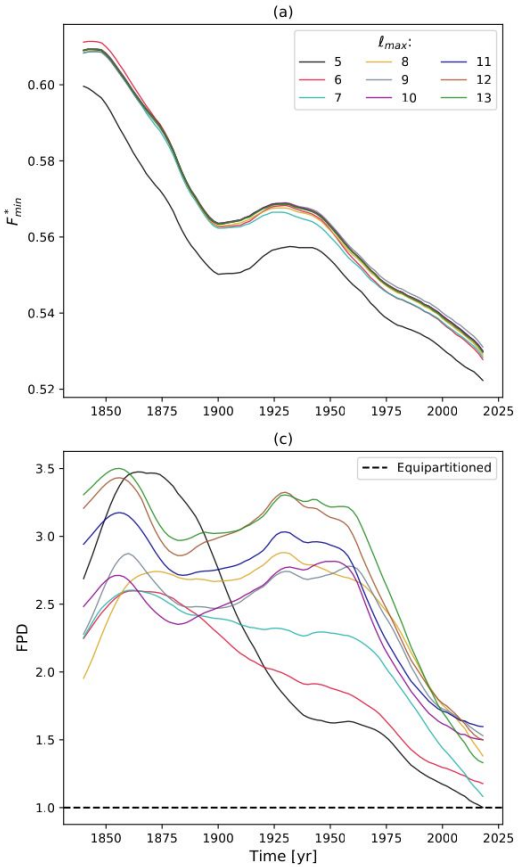

Time-averages:

- F^*_{min} is weakly dependent on ℓ_{max}
- FPD increases (though not monotonically) with ℓ_{max}

Time-evolution of the geomagnetic power spectra for small scales

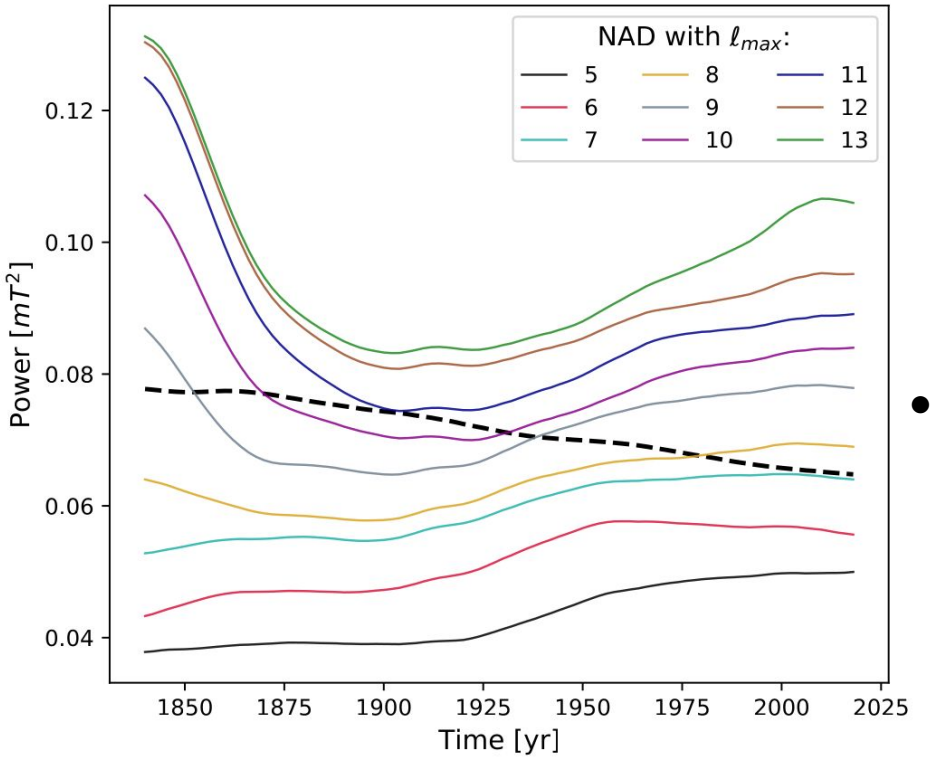

- Faster decrease of small scales than of the axial dipole (dashed line) in the beginning of the historical era